

# Dynamics of Kinks in One- and Two- Dimensional Hyperbolic Models with Quasi-Discrete Nonlinearities

**Horacio G. Rotstein<sup>\*</sup>, Anatol Zhabotinsky, Irving Epstein**

Department of Chemistry and Volen Center for Complex Systems,  
Brandeis University, MS 015, Waltham, MA 02454-9110, USA

February 5, 2020

## Abstract

We study the evolution of fronts in the Klein-Gordon equation when the nonlinear term is non-homogeneous. Extending previous works on homogeneous nonlinear terms, we describe the derivation of an equation governing the front motion, which is strongly nonlinear, and, for the two-dimensional case, generalizes the damped Born-Infeld equation. We study the motion of one- and two-dimensional fronts, finding that the dynamics is richer than in the homogeneous reaction term case.

## 1 Introduction

In the last few years, partial differential equations with discrete nonlinearities have been used to model phenomena in fields ranging from physics to biology, including the study of

---

<sup>\*</sup>E-mail: horacio@cs.brandeis.edu

pinning of dislocation motions in crystals, breathers in nonlinear crystal lattices, Josephson junction arrays and the biophysical description of calcium release waves [?, ?, ?, ?, ?, ?, ?, ?, ?, ?, ?, ?, ?, ?, ?]. Recently, the discrete one-dimensional stationary version of the Klein-Gordon equation

$$\phi_{tt} + \gamma \phi_t = D \phi_{xx} + \alpha \sum_k \delta(x - x_k) [f(\phi) + h], \quad (1)$$

with  $\gamma = 0$  has been analyzed by Flach and Kladko [?] (see also references therein). In (1)  $\phi$  is an order parameter, the non-negative constant  $\gamma$  is the dissipation coefficient and the positive constants  $D$  and  $\alpha$  are the diffusion coefficient and the amplitude of the discrete nonlinearity, respectively. The function  $f$  is a bistable function (the derivative of a double well potential having the two equal minima); i.e., a real odd function with positive maximum equal to  $\phi^*$ , negative minimum equal to  $-\phi^*$  and precisely three zeros in the closed interval  $[a_-, a_+]$  located at  $a_-$ ,  $a_0$  and  $a_+$ . For simplicity and without loss of generality we will consider in our analysis  $a_- = -1$ ,  $a_0 = 0$  and  $a_+ = 1$ . The prototype example is  $f(\phi) = (\phi - \phi^3)/2$ . The constant  $h$ , assumed to be small in absolute value, specifies the difference of the potential minima of the system; i.e.,  $f(\phi) + h$  is the derivative of a double well potential with one local minimum and one global minimum. Note that (1) reduces to the Klein-Gordon equation when  $\sum_k \delta(x - x_k)$  is replaced by a constant with appropriate rescaling. In [?] a first order perturbation calculation for the heteroclinic orbits of the corresponding stationary kink solution for (1) was presented. Kink solutions, connecting the two local minima of the double well potential, were also obtained for the sine-Gordon case,  $f(\phi) = -\sin(\phi)$ , and the Klein-Gordon case,  $f(\phi) = (\phi - \phi^3)/2$ . Both are particular cases of the function  $f(\phi)$  as defined above. Note that the sine-Gordon case is equivalent to the derivative of a double well potential in a restricted domain of definition.

In this manuscript, we study the dynamics of kinks for a quasi-discrete version of the Klein-Gordon equation

$$\phi_{tt} + \gamma \phi_t = D \Delta \phi + \alpha \beta(x, y) [f(\phi) + h], \quad (2)$$

in a bounded region  $\Omega \subset R^n$ ,  $n = 1, 2$  with smooth boundary  $\partial\Omega$  for Neumann boundary conditions on  $\partial\Omega$ . Equation (2) reduces to (1) when  $\beta$  is one-dimensional and  $\beta(x) = \sum_k \delta(x - x_k)$ . Although the analysis presented below will be valid for a general class of positive differentiable functions  $\beta$ , we have in mind some particular cases which approximate a distribution of discrete nonlinearities for large  $\eta$ , a positive constant defined below.

Case 1) There is a sequence of points on the real line,  $x_k$ ,  $k = 1, \dots, N$ , with  $N$  finite or infinite, where the function  $\beta$  reaches a maximum,

$$\beta(x) = \sum_{k=1}^N e^{-\eta(x-x_k)^2}. \quad (3)$$

Case 2) There is a sequence of lines in the plane,  $y_k$ ,  $k = 1, \dots, N$ , with  $N$  finite or infinite, where the function  $\beta$ , independent of  $x$ , reaches a maximum,

$$\beta(x, y) = \sum_{k=1}^N e^{-\eta(y-y_k)^2}. \quad (4)$$

Case 3) There is a sequence of points in the plane,  $(x_k, y_j)$ ,  $k = 1, \dots, N$ ,  $j = 1, \dots, M$  with  $N$  and  $M$  finite or infinite, where the function  $\beta$  reaches a maximum,

$$\beta(x, y) = \sum_{k=1}^N \sum_{j=1}^M \sigma(x - x_k, y - y_j; \eta), \quad \text{where} \quad \sigma(x, y; \eta) = e^{-\eta(x^2+y^2)}. \quad (5)$$

Case 4) There is a sequence of circles in the plane,  $\rho = \rho_k$ ,  $k = 1, \dots, N$ , with  $N$  finite or infinite, and where  $\rho$  represents the radial polar coordinate, where the function  $\beta$  reaches a maximum,

$$\beta(\rho) = \sum_{k=1}^N e^{-\eta(\rho-\rho_k)^2}. \quad (6)$$

We refer to the points  $x_k$  and  $(x_k, y_j), k = 1, \dots, N, j = 1, \dots, M$  as quasi-discrete (QD) sites and to the stripes  $y = y_k$  and circles  $\rho = \rho_k, k = 1, \dots, N$  as quasi-semi-discrete (QS) sites. We define  $d$  to be the minimum distance between two adjacent QD or QS sites. Note that the function  $\beta$  can be chosen to depend not only on the spatial variable but also on  $t$ . The specific form of  $\beta(x, y, t)$  will depend on the particular model. One might, for example, have the product of a spatially dependent function  $\beta(x, y)$  with a probabilistic time-dependent function.

For (2) we define the following dimensionless variables and parameters

$$\hat{x} = \frac{x}{d}, \quad \hat{y} = \frac{y}{d}, \quad \hat{t} = \frac{\sqrt{D}}{d} t \quad (7)$$

and

$$\epsilon = \sqrt{\frac{D}{\alpha}} \frac{1}{d}, \quad \hat{\gamma} = \frac{\gamma d}{\sqrt{D}}, \quad \hat{\eta} = \eta d^2, \quad \hat{h} = \frac{h}{\epsilon}. \quad (8)$$

Substituting (7) and (8) into (2) and dropping the  $\hat{\phantom{x}}$  from the variables and parameters

$$\epsilon^2 \phi_{tt} + \epsilon^2 \gamma \phi_t = \epsilon^2 \Delta \phi + \beta(x, y) [f(\phi) + \epsilon h]. \quad (9)$$

We will consider the case  $0 < \epsilon \ll 1$ ; i.e., when diffusion is slow,  $d$  is large or  $\alpha$  is large, and there is a small dissipation.

The homogeneous version of (9),

$$\epsilon^2 \phi_{tt} + \epsilon^2 \gamma \phi_t = \epsilon^2 \Delta \phi + f(\phi) + h, \quad (10)$$

possesses a travelling kink solution. The point on the line (for  $n = 1$ ) or the set of points in the plane (for  $n = 2$ ) for which the order parameter  $\phi$  vanishes are called the interface or front of the system. For (10) the front moves according to an extended version of the Born-Infeld equation [?, ?]

$$(1 - s_t^2) s_{xx} + 2 s_x s_t s_{xt} - (1 + s_x^2) s_{tt} - \gamma s_t (1 + s_x^2 - s_t^2) - \hat{h} (1 + s_x^2 - s_t^2)^{\frac{3}{2}} = 0, \quad (11)$$

where  $\hat{h}$ , proportional to  $h$ , will be defined later. Planar fronts moving according to (11) with  $\gamma = \hat{h} = 0$  (no dissipation and both phases with equal potential) move with a constant velocity equal to their initial velocity. For other values of  $\gamma$  or  $\hat{h}$ , fronts move with a velocity that asymptotically approaches  $-\hat{h}/(\gamma^2 + \hat{h}^2)^{\frac{1}{2}}$  as long as the initial velocity is bounded from above by 1 in absolute value. Linear perturbations to these planar fronts decay, either in a monotonic or an oscillatory way, to zero as  $t \rightarrow \infty$  [?]. Circular interfaces moving according to (11) with  $h > 0$  shrink to a point in finite time [?, ?]. If  $h < 0$ , then circles shrink to points for some initial conditions and for others they grow unboundedly. Neu [?] showed that for  $\gamma = h = 0$ , closed kinks can be stabilized against collapse by the appearance of short wavelength, small amplitude waves. For the more general case, two situations are possible. Either linear perturbations to a circle decay and curves shrink to a point in finite time or they are still present at the shrinkage point of the circle. Note that Equation (11) expressed in terms of its kinematic and geometric properties reads [?]

$$\frac{dv}{dt} + \gamma v (1 - v^2) - \kappa (1 - v^2) + \hat{h} (1 - v^2)^{\frac{3}{2}} = 0, \quad (12)$$

where  $\kappa$  is the curvature of the front and  $dv/dt$  is the "Lagrangian" time derivative of  $v$  which is calculated along the trajectory of the interfacial point moving with the normal velocity  $v$  [?].

One of the goals of this paper is to determine whether the dynamic behavior of kinks in (9) differs from its homogeneous (discrete) nonlinearity counterpart (10). For the overdamped version of equation (2), which is a parabolic bistable equation, it has been shown that there are essential differences between the homogeneous and non-homogeneous (discrete) cases, in that latter exhibits propagation failure [?, ?, ?, ?, ?].

In Section 2 we present an equation of motion for the front in equation (9), and we describe briefly the method by which it was derived. This equation generalizes equation (11) with the strong nonlinearity accounting for the influence of the function  $\beta$  on the front motion. In Section 3 we study the evolution of one-dimensional fronts. We show that for  $h = 0$  the function  $\beta$  acts as a "potential function" for the motion of the front; i.e., a front initially placed between two maxima of  $\beta$  asymptotically approaches the intervening minimum. When  $h \neq 0$ , fronts that start between two maxima of  $\beta$  asymptotically approach an equilibrium point determined by  $h$  and  $\beta$ , producing a kink propagation failure. In Section 4 we study the evolution of two-dimensional fronts with radial symmetry. We find that when there is no dissipation circles can shrink to a point in finite time, grow unboundedly or their radius can oscillate, depending on the initial conditions. When dissipation effects are present, the oscillations decay spirally or not depending of the value of  $\gamma$ . The final result is the stabilization of the circular domain of one phase inside the other phase. Our conclusions appear in Section 5.

## 2 Front Dynamics: The Equation of Motion

For (9) and the law of motion of the interface in two dimensions is given by

$$(1 - s_t^2) s_{xx} + 2 s_x s_t s_{xt} - (1 + s_x^2) s_{tt} - \gamma s_t (1 + s_x^2 - s_t^2) - \frac{\beta_y(x, s) - \beta_x(x, s) s_x + \beta_t(x, s) s_t}{2 \beta(x, s)} (1 + s_x^2 - s_t^2) - \hat{h} \beta^{\frac{1}{2}}(x, s) (1 + s_x^2 - s_t^2)^{\frac{3}{2}} = 0, \quad (13)$$

where  $y = s(x, t)$  is the Cartesian description of the interface and  $\hat{h}$  is proportional to  $h$  as will be explained later. Equation (13) was obtained by carrying out a non-rigorous but self-consistent singular perturbation analysis for  $\epsilon \ll 1$ , treating the interface as a moving internal layer of width  $O(\epsilon)$ . We focused on the dynamics of the fully developed layer, and

not on the process by which it was generated. The method that we applied is similar to that used in [?] and [?] for the study of the evolution of kinks in both the nonlinear wave equation (10) and the Allen-Cahn equation with quasi-discrete sources of reaction (the overdamped version of (2)). The basic assumptions made were:

- For small  $\epsilon \geq 0$  and all  $t \in [0, T]$ , the domain  $\Omega$  can be divided into two open regions  $\Omega_+(t; \epsilon)$  and  $\Omega_-(t, \epsilon)$  by a curve  $\Gamma(t; \epsilon)$ , which does not intersect  $\partial\Omega$ . This interface, defined by  $\Gamma(t; \epsilon) := \{x \in \Omega : \phi(x, t; \epsilon) = 0\}$ , is assumed to be smooth, which implies that its curvature and its velocity are bounded independently of  $\epsilon$ .
- There exists a solution  $\phi(x, t; \epsilon)$  of (2), defined for small  $\epsilon$ , for all  $x \in \Omega$  and for all  $t \in [0, T]$  with an internal layer. As  $\epsilon \rightarrow 0$  this solution is assumed to vary continuously through the interface, taking the value 1 when  $x \in \Omega_+(t; \epsilon)$ ,  $-1$  when  $x \in \Omega_-(t, \epsilon)$ , and varying rapidly but smoothly through the interface.
- The curvature of the front is small compared to its width.

As a first stage in the derivation of equation (13) we define near the interface a new variable  $z = (y - s)/\epsilon$  which is  $\mathcal{O}(1)$  as  $\epsilon \rightarrow 0$  and then express equation (9) in terms of this new variable. Next we expand  $\phi$  and  $\beta$  asymptotically in a power series in  $\epsilon$  and substitute these expansions into the differential equation. After equating the coefficients of corresponding powers of  $\epsilon$ , we obtain two equations. The first can be reduced to an equation of the type  $\Phi_{zz}^0 + f(\Phi^0) = 0$  which has to satisfy  $\Phi^0(0) = 0$  and  $\Phi^0(\pm 1) = \pm 1$ , giving a kink solution. Here  $\Phi^0$  represents the leading order term of the order parameter  $\phi$  in terms of  $z$ . The second problem is a linear non-homogeneous second order ODE. Equation (13) is obtained by applying the solvability condition (Fredholm alternative) after defining  $\hat{h} := h [\Phi^0(+\infty) - \Phi^0(-\infty)] / \int_{-\infty}^{\infty} (\Phi_z^0)^2 dz$ . Note that for  $f(\phi) = (\phi - \phi^3)/2$  (Ginsburg-Landau theory),  $\Phi^0(z) = \tanh \frac{z}{2}$  and  $\hat{h} = 3 h$  whereas for  $f(\phi) = \sin \phi$  (sine-Gordon),  $\Phi^0(z) = 4 \tan^{-1} e^z - \pi$  and  $\hat{h} = \frac{\pi}{4} h$ .

### 3 Front Motion in 1D

For a one-dimensional system, equation (13) reads

$$s_{tt} + \gamma s_t (1 - s_t^2) + \frac{\beta'(s)}{2\beta(s)}(1 - s_t^2) + \hat{h} \beta^{\frac{1}{2}}(s) (1 - s_t^2)^{\frac{3}{2}} = 0. \quad (14)$$

We concentrate on functions  $\beta$  of the form (3), although the same analysis can be done for a general differentiable function. We define  $u = s$  and  $v = s_t$  obtaining

$$\begin{cases} u_t = v, \\ v_t = -\gamma v (1 - v^2) - \frac{\beta'(u)}{2\beta(u)}(1 - v^2) - \hat{h} \beta^{\frac{1}{2}}(u) (1 - v^2)^{\frac{3}{2}}. \end{cases} \quad (15)$$

The fixed points of (15) are  $(u_0, 0)$ , where  $u_0$  satisfies  $g(u) = \beta'(u) + 2\hat{h}\beta^{\frac{3}{2}}(u) = 0$ .

The trace,  $\tau$ , and determinant,  $\Delta$ , of matrix of the linearized system are  $\tau = -\gamma$  and  $\Delta = [\beta''(u_0)\beta(u_0) - \beta'^2(u_0)] / 2\beta^2(u_0) + \hat{h}\beta'(u_0)/[2\beta^{\frac{1}{2}}(u_0)]$ , respectively. If  $\hat{h} = 0$  then the fixed points are the maxima (unstable) and minima (stable) of  $\beta(u)$ . Thus, a front initially between two maxima of  $\beta$  will move and asymptotically approach the intervening minimum.

When there is no dissipation, this behavior is in contrast with the homogeneous case (11) where, as was pointed out in the introduction, fronts move with a constant velocity equal to their initial velocity. In the non-homogeneous case, we can predict the final position of the front from the structure of  $\beta$ . In order to understand the behavior of  $g(u)$  as  $\hat{h}$  increases above zero we consider a function  $\beta(u)$  with a single peak at 0; i.e.,  $\beta(u) = e^{-\eta u^2}$ . This function will approximate the more general (3) if  $\eta \gg 1$ , so that the influence of peaks on one another is very small. In this case  $g(u) = -2e^{-\eta u^2}[\eta u - \hat{h} e^{-\frac{\eta u^2}{2}}]$ . For  $\hat{h} = 0$ ,  $g(u)$  vanishes at  $u = 0$  and it is positive for  $u > 0$  and negative for  $u < 0$ . As  $\hat{h}$  moves away from zero,  $\hat{u}$ , the root of  $g(u)$ , will be given by the solution of  $\eta u - \hat{h} e^{-\frac{\eta u^2}{2}} = 0$ , an equation that always has a solution. If  $\hat{h} > 0$ , then  $\hat{x} > 0$ , and  $g(u)$  is positive for  $x > \hat{x}$  and negative for  $x < \hat{x}$ . If  $\hat{h} < 0$ , then  $\hat{x} < 0$ . As an illustration, We can see the shape of  $g(u)$  as  $\hat{h}$  increases in Figure 1. In summary, as  $\hat{h}$  increases or decreases the behavior of the front is similar to



the case  $\hat{h} = 0$ , in contrast to the classical homogeneous case (11) where, as noted in Section 1, fronts with an initial velocity whose absolute value is bounded from above by 1, move with a velocity that asymptotically approaches  $-\hat{h}/(\gamma^2 + \hat{h}^2)^{\frac{1}{2}}$ .

## 4 Front Motion in 2 D

The analysis of front motion in two dimensions governed by (13) with a function  $\beta$  of type (4) reduces to the analysis of one-dimensional front motion, and we shall not consider this case further. For radially symmetric functions,  $\beta = \beta(\rho)$ , and radially symmetric fronts, equation (13) for the radial coordinate  $\rho$  of the front reads

$$\rho_{tt} + \left(\gamma \rho_t + \frac{1}{\rho}\right) (1 - \rho_t^2) + \frac{\beta'(\rho)}{2 \beta(\rho)} (1 - \rho_t^2) + \beta^{\frac{1}{2}}(\rho) \hat{h} (1 - \rho_t^2)^{\frac{3}{2}}, \quad (16)$$

We define  $u = \rho$  and  $v = \rho_t$  obtaining

$$\begin{cases} u_t = v, \\ v_t = -\left[\gamma v + \frac{1}{u} + \frac{\beta'(u)}{2 \beta(u)} + \hat{h} \beta^{\frac{1}{2}}(u) (1 - v^2)^{\frac{1}{2}}\right](1 - v^2). \end{cases} \quad (17)$$

The lines  $v = \pm 1$  are trajectories of (17) in the corresponding phase plane. They define a region  $D$  with the property that every curve starting in this region remains inside it for all future time. We confine our analysis to  $u > 0$ . We analyze here the case  $\hat{h} = 0$ . The fixed points of (17) are  $(u_0, 0)$ , where  $u_0$  are solutions (if they exist) of  $2 \beta(u) + u \beta'(u) = 0$ . The trace,  $\tau$ , and the Determinant,  $\Delta$ , of the matrix of the linearized system are given by  $\tau = -\gamma$  and  $\Delta = -1/u_o^2 + [\beta''(u_0) \beta(u_0) - \beta'^2(u_0)] / 2 \beta^2(u_0)$  respectively. The simplest case is  $\beta(\rho) = e^{-\eta(\rho-\rho_1)^2}$  for a given  $\rho_1 > 0$ . For this case  $u_0 = \left(\eta \rho_1 + \sqrt{\eta^2 \rho_1^2 + 4 \eta}\right) / 2 \eta$  and  $(u_0, 0)$  is a saddle point. For (4) with  $\eta = 50$  and  $N = 2$ ,  $\rho_1 = 0.5$  and  $\rho_2 = 1.5$ , we calculated the fixed points of (17) using the Newton-Raphson method with a tolerance of 0.0001. They are  $z_1 = 0.537228$ ,  $z_2 = 0.999165$  and  $z_3 = 1.513217$ . The corresponding values of  $\Delta$  are  $\Delta(z_1) = -53.464832$ ,  $\Delta(z_2) = 1196.824463$  and  $\Delta(z_3) = -50.436714$ . Then

$z_1$  and  $z_3$  are saddle points, and  $z_2$  is stable. Since the discriminant,  $\Lambda = \tau^2 - 4 \Delta$  of  $z_2$ , is  $-4787.297852 < 0$ ,  $z_2$  is a neutrally stable center for  $\gamma = 0$ , a stable spiral for  $0 < \gamma \leq \gamma_0$  and a stable node for  $\gamma > \gamma_0$ , where  $\gamma_0$  is the value of  $\gamma$  for which  $\Lambda = 0$ .

For the case  $\gamma = 0$ , dividing the second equation in (17) by the first and solving one obtains

$$c^2 u^2 \beta(u) + v^2 = 1, \quad (18)$$

where  $c^2 = (1 - v_i^2)/(u_i^2 \beta(u_i))$  and  $(u_i, v_i)$  are the initial conditions. In Figure 2 we present a graph of (18) for  $\beta$  given by (4) with  $N = 2$ ,  $\rho_1 = 0.5$ ,  $\rho_2 = 1.5$   $\eta = 50$  (a) and  $\eta = 10$  (b). We observe that there are shrinking trajectories, oscillatory trajectories and growing trajectories in contrast with the homogeneous case where all trajectories are shrinking trajectories given by  $c^2 u^2 + v^2 = 1$  with  $c^2 = (1 - v_i^2)/u_i^2$  [?]. As  $\eta$  decreases, the oscillatory trajectories disappear, leaving growing trajectories, which will ultimately vanish as  $\eta \rightarrow 0$ .

In order to study more generally the behavior of the system away from the fixed points we can see in Figure 3 the phase plane for  $\gamma = 0$  (a) and  $\gamma = 1$  (b). The dashed lines are the nullclines of the system and the "o" are its fixed points. The trajectories were calculated solving (17) using a Runge-Kutta method of order four. We observe there that there are different situations according to the initial conditions. In Figure 3-a (no dissipation), trajectories  $A$ ,  $B$  and  $C$  correspond to circles that shrink to a point in finite time. If their initial velocity is positive, then their radius grows initially to a value bounded by  $z_1$  before shrinkage takes place. Trajectories  $D$  and  $J$  also correspond to a circles that finally shrink to a point in finite time. In the case of  $D$ , although the initial conditions are close to those of trajectory  $C$ , the dynamics is very different. In addition to shrinkage, trajectories can display unbounded growth, represented by trajectory  $G$ , and periodic behaviour, represented by trajectories  $E$  and  $F$ . Trajectories  $H$  and  $I$  also correspond to circles growing unboundedly, but if the initial velocity is negative they shrink to a valued bounded from below by  $z_3$  and then they start growing. In Figure 3-b ( $\gamma = 1$ ) we see that trajectories  $A$ ,  $B$  and  $C$  correspond to circles

that shrink to points in finite time after growing to a radius bounded by  $z_1$ . Trajectory  $D$  also shrinks to a point in finite time, but it grows initially to a radius bounded from above by  $z_3$  and from below by  $z_2$ . As we pointed out before, as a consequence of dissipation ( $\gamma \neq 0$ )  $z_2$  is a stable spiral. We see that trajectory  $E$  spirals into  $z_2$ , and there are no longer periodic trajectories. For  $N > 2$  we expect the phase plane analysis to be similar to that presented here. In contrast with the homogeneous nonlinear wave equation, where any circular front shrinks to a point in finite time, the nonhomogeneous version (13) presents a very rich dynamics with periodic motion and stabilization of circular domains of one phase inside the other.

In the absence of dissipation there are two "forces" responsible for the motion of the front: the curvature of the circular front,  $1/\rho$ , and the "potential function"  $\beta$ . For initial conditions near enough to the minimum of  $\beta$  the two "forces" balance and oscillations are possible. When dissipation is present that "balance" is lost, and the oscillations decay.

## 5 Conclusions

In this manuscript we have presented equation (13) as governing the evolution of a fully developed front in a nonhomogeneous version of the nonlinear wave equation, (9), when  $\epsilon \ll 1$ . This equation generalizes the damped version of the Born-Infeld equation (11) to include the effects of stronger nonlinearities and accounts for the influence of the nonhomogeneous nonlinear term on the motion of the front. The motion of interfaces according to (13) is qualitatively different from that of the homogeneous counterpart given by (11). This difference arises primarily from the fact that the function  $\beta$  acts as a "potential function" for the motion of the front. For the one dimensional case, an initial front initially placed between two maxima of  $\beta$  (which for a homogeneous nonlinear term will move with a velocity that asymptotically approaches  $-\hat{h}/(\gamma^2 + \hat{h}^2)^{\frac{1}{2}}$  as long as the initial velocity bounded from

above by 1 in absolute value asymptotically approaches a point depending on  $\hat{h}$  and on the structure of  $\beta$ . For the radially symmetric two-dimensional case, the dynamics is richer than in the homogeneous counterpart, where for  $\hat{h} = 0$  circles shrink to point in finite time. In the absence of dissipation, circles can shrink to a point in finite time, grow unboundedly or their radius oscillates, depending on the initial conditions. When dissipation effects are present, the oscillations decay, spirally or not, depending on the value of  $\gamma$ . The final result is the stabilization of a circular domain of one phase inside the other phase.

The evolution of circular interfaces in more complicated arrangement of QD sites and the evolution of more complicated fronts like convex closed curves calls for further research. We hope to address this questions in a forthcoming paper.

Acknowledgement: We thank the Chemistry Division of the National Science Foundation for support of this work.

### Captions

Figure 1:

- a) Graph of  $\beta(u)$  for  $\eta = 1000$ ,  $x_1 = 2$ ,  $x_2 = 1$ ,  $x_3 = 0$  and  $x_4 = -1$ ,  $x_5 = -2$ .
- b) Graph of  $g(u)$  for  $\eta = 1000$ ,  $h = 0$ ,  $x_1 = 2$ ,  $x_2 = 1$ ,  $x_3 = 0$  and  $x_4 = -1$ ,  $x_5 = -2$ .
- c) Graph of  $g(u)$  for  $\eta = 1000$ ,  $h = 10$ ,  $x_1 = 2$ ,  $x_2 = 1$ ,  $x_3 = 0$  and  $x_4 = -1$ ,  $x_5 = -2$ .
- d) Graph of  $g(u)$  for  $\eta = 1000$ ,  $h = 20$ ,  $x_1 = 2$ ,  $x_2 = 1$ ,  $x_3 = 0$  and  $x_4 = -1$ ,  $x_5 = -2$ .

The points  $x_k$  are the maxima of  $\beta(u)$ .

Figure 2:

Graph of (18) with  $\beta$  given by (4) with  $N = 2$ ,  $\rho_1 = 0.5$ ,  $\rho_2 = 1.5$  and

- a)  $\eta = 50$ .
- b)  $\eta = 10$ .

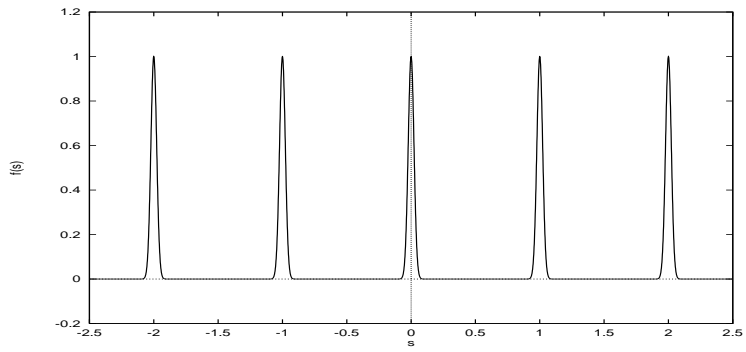
Figure 3:

Phase plane for (17) with  $\beta$  given by (4) with  $N = 2$ ,  $\rho_1 = 0.5$ ,  $\rho_2 = 1.5$ ,  $\eta = 50$  and  $\hat{h} = 0$ .

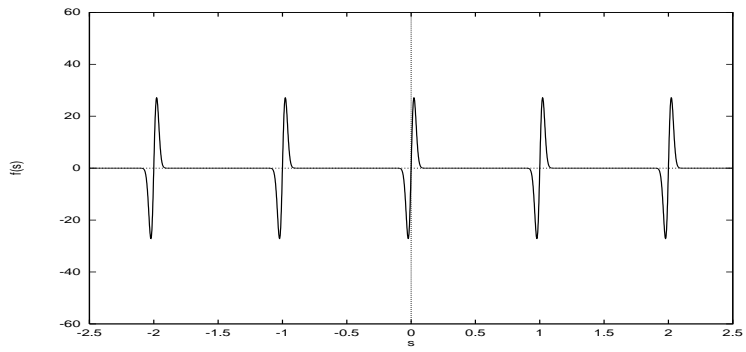
The dashed lines are the nullclines of the system and the "o" are its fixed points.

- a)  $\gamma = 0$ .
- b)  $\gamma = 1$ .

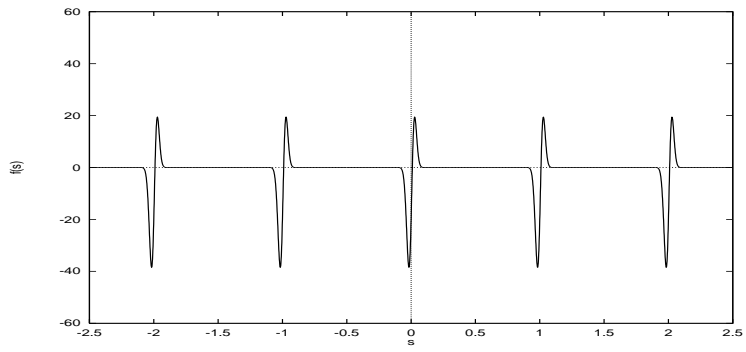
(a)



(b)



(c)



(d)

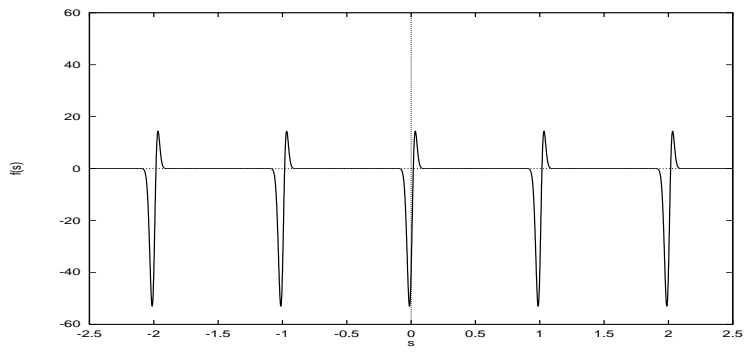
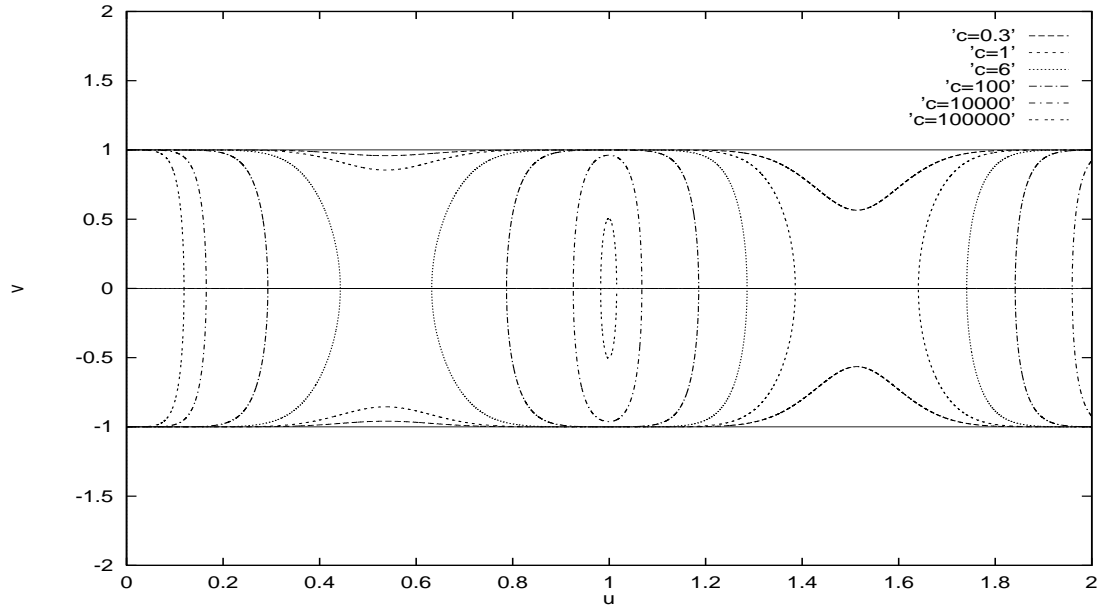


Figure 1:

(a)



(b)

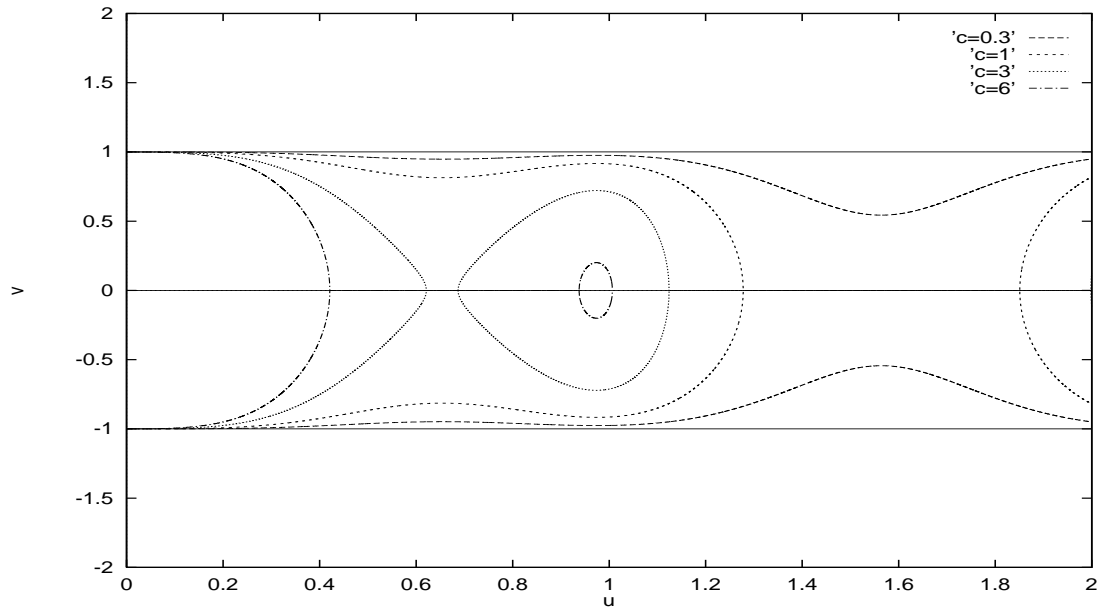
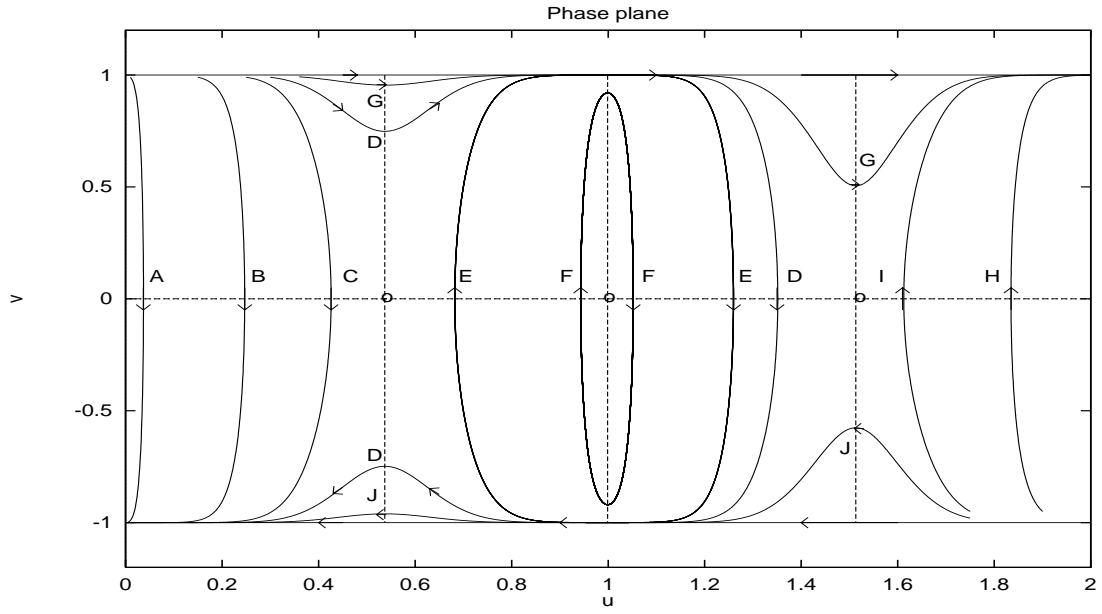


Figure 2:

(a)



(b)

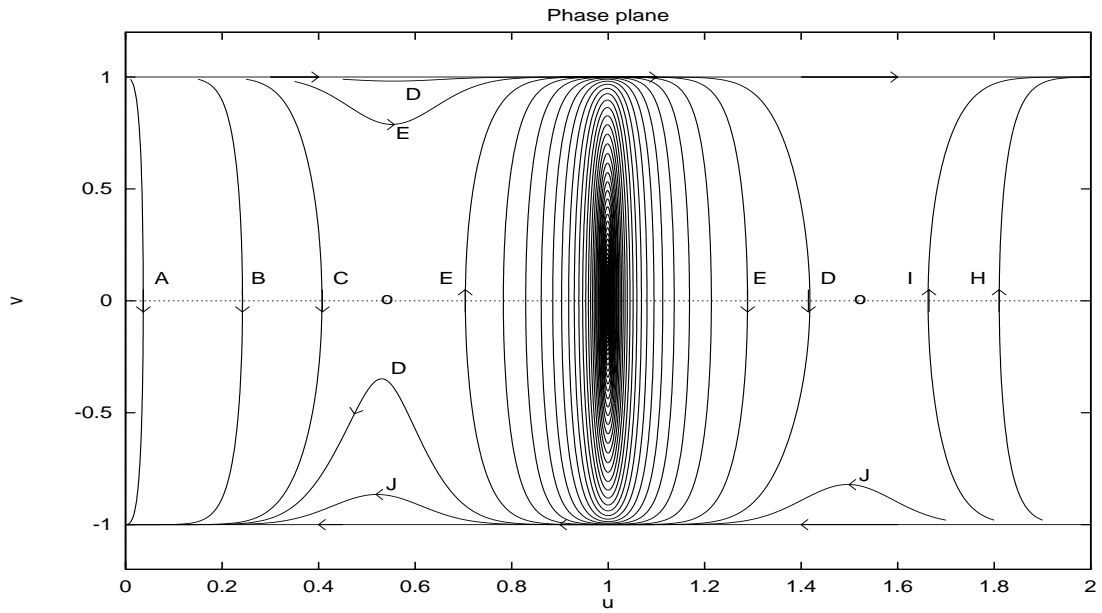


Figure 3: